

Fast-Flow Kinetic Studies of Methane Reactions with Atomic Oxygen at Room Temperature

R. V. Serauskas and R. A. Keller

Institute of Gas Technology, IIT Center
Chicago, Illinois

I. Introduction

Many contributions to kinetic rate knowledge have resulted from premixed flame studies.^{1,2,3} A flame, consisting of a multi-reaction complex medium, lends

1. R. M. Fristrom, and A. A. Westenberg, "Flame Structure," McGraw-Hill, New York (1965).
 2. S. W. Benson, "The Foundations of Chemical Kinetics," McGraw-Hill, New York, 276 (1960).
 3. N. Basco and R.G.W. Norrish, *Can. J. Chem.* **38**, 1769 (1960).
- itself to unambiguous kinetic analysis only with difficulty. Specifically, the more recent flame studies of combustible methane mixtures⁴ have directed much inter-
4. R. M. Fristrom, C. Grunfelder, and S. Favin, *J. Phys. Chem.* **64**, 1386 and 1393 (1960).

est of late toward the elementary reactions in the methane oxidation scheme. New and improved techniques for the study of atom and radical reactions have led to renewed kinetic studies which have confirmed some earlier results and have been at odds with others. The addition of various chemically perturbing agents to the O-atom/CH₄ system, for example, allow for the study of some elementary oxidation reactions at room temperature by the more convenient and unambiguous flow-discharge techniques. However the results in all cases have not been uniform, especially in systems containing oxygen.⁵

5. F. Kaufman, in "Progress in Reaction Kinetics," Vol. 1 (ed. G. Porter), Pergamon Press, New York, 1 (1961).

In this work, a number of methane-oxygen reactions have been studied employing a fast-flow reaction system, coupled directly with a Bendix model 3015 time-of-flight mass spectrometer. N and H-atom titrations as well as Woods-Bonhoeffer discharges are employed in generating the active species.

II. Experimental

The reaction system employed is depicted schematically in Figure 1. A Woods-Bonhoeffer discharge-flow system is in train with a Bendix model 3015 time-of-flight mass spectrometer. Atoms or radicals enter in the central annular space in the reaction train. Reactants enter through the central tube fitted with a Teflon "Swage" gland to permit movement along the reaction train axis. In this way, the distance of the mixing region from the molecular leak (aluminum foil disk with an 0.005 inch pinhole) can be varied. A 40 liter/sec Stokes' pump throttled through a linear flow velocity of about 10 meters/sec and a reaction region pressure in the 10 to 1000 millitorr range. Knowing the volumetric flow rate, v , and the diameter, d , of the reactor, the distance, z , of the tube mouth from the TÖF sampling leak can be related to the time variable, t , in an absolute fashion by the relation:

$$t = \left(\frac{\pi d^2}{4v}\right) z^{-1}$$

This reaction holds strictly for the case of a cylindrical reactor and laminar flow.⁵ The methane, used without further purification, was Matheson Ultra-High Purity grade. Matheson Research grade HCl was employed in the catalytic study. Matheson High Purity grade NO₂ was redistilled in vacuo for use in the generation of OH radicals. The oxygen used was Ultra-High Purity grade Matheson, employed without further purification.

Oxygen atoms were generated by two methods: (1) the discharge of a 1 to 9 O₂/Ar mixture (2) the very rapid gas-phase titration of NO by N atoms (N + NO →

N_2+O), the N atoms being generated by discharging N_2 . The hydroxyl radicals were generated by the rapid gas phase titration of NO_2 with H atoms ($H+NO_2 \rightarrow NO+OH$), the H atoms being generated by discharge of a 5% $H_2/95\%$ Ar mixture containing a trace of water in order to aid dissociation (The walls of the reaction train were coated with phosphoric acid to give low, reproducible wall-recombination effects.) In all cases the temperature remained within 1° of $298^\circ K$.

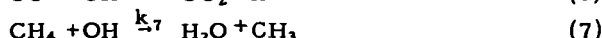
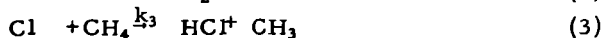
III. Results and Discussion

A. Methane-O-atom Reaction with HCl Catalyst

At room temperature the reaction between methane and atomic oxygen is extremely slow because the reaction has a heat of activation between 8-9 kcal/g-mole.¹ Consequently, if one wished to study the reaction, the investigation must be conducted at elevated temperatures or a suitable catalyst must be added for room temperature studies.

We selected hydrogen chloride gas as a catalyst for this study because it is known to accelerate the reaction between methane and atomic nitrogen.

The following reactions may be considered in this system:



This reaction scheme yields a series of 12 simultaneous differential equations that are extremely difficult to solve analytically.

As a first approximation, we might eliminate all of the reactions with an energy of activation of 8 kcal/g-mole or more. At $300^\circ K$, the difference in rate between a reaction with $E_a = 4$ kcal/g-mole and one with 8 kcal/g-mole is a factor of about 10^3 . Thus, two reactions with approximately equal reactant concentrations and frequency factors will differ in rate by 1000 if they have such an activation energy difference.

Using this criterion, Table I^{1,6} shows that Reaction 7 through 11 can be eliminated from the reaction scheme. K. Schofield, *Planet. Space Sci.* 15, 643 (1967).

We will show later that an error has apparently been introduced by eliminating Reaction 9. The concentration of H atoms apparently is sufficiently high to offset the activation energy difference.

A second approximation involves the "steady-state assumption." This assumption specifies that the rate expressions for all of the active species be set equal to zero. For example, the rate of formation of chlorine atoms is as follows:

$$\frac{d(Cl)}{dt} = k_1(HCl)(O) - k_3(Cl)(CH_4) \quad (13)$$

Using the steady-state assumption yields the following equation:

$$k_1(HCl)(O) - k_3(Cl)(CH_4) = 0 \quad (14)$$

The following equations are obtained by using the steady-state assumption for CH_2 , CH_3 , and OH :

$$k_4(\text{CH}_3)(\text{O}) - k_5(\text{CH}_2)(\text{O}) = 0 \quad (15)$$

$$k_3(\text{Cl})(\text{CH}_4) - k_4(\text{CH}_3)(\text{O}) = 0 \quad (16)$$

$$k_1(\text{HCl})(\text{O}) - k_2(\text{OH})(\text{O}) + k_4(\text{CH}_3)(\text{O}) - k_6(\text{CO})(\text{OH}) = 0 \quad (17)$$

This series of four algebraic equations can now be solved for the concentrations of the active species:

$$(\text{Cl}) = \frac{k_1(\text{HCl})(\text{O})}{k_3(\text{CH}_4)} \quad (18)$$

$$(\text{CH}_2) = \frac{k_1(\text{HCl})}{k_5} \quad (19)$$

$$(\text{CH}_3) = \frac{k_1(\text{HCl})}{k_4} \quad (20)$$

$$(\text{OH}) = \frac{2k_1(\text{HCl})(\text{O})}{k_2(\text{O}) + k_6(\text{CO})} \quad (21)$$

The rates of the reactions of O, CO, and CO₂ can now be written and simplified using the above expressions for the concentrations of the active species.

$$\frac{d(\text{O})}{dt} = -3k_1(\text{HCl})(\text{O}) - \frac{2k_1k_2(\text{HCl})(\text{O})^2}{k_2(\text{O}) + k_6(\text{CO})} \quad (22)$$

$$\frac{d(\text{CO})}{dt} = k_1(\text{O})(\text{HCl}) - \frac{2k_1k_6(\text{HCl})(\text{O})(\text{CO})}{k_2(\text{O}) + k_6(\text{CO})} \quad (23)$$

$$\frac{d(\text{CO}_2)}{dt} = \frac{2k_1k_6(\text{HCl})(\text{O})(\text{CO})}{k_2(\text{O}) + k_6(\text{CO})} \quad (24)$$

For the conditions of this study, $(\text{CO}) < 1/5 (\text{O})$ so that $k_2(\text{O}) \gg k_6(\text{CO})$. The rate expression for the disappearance of atomic oxygen is, therefore:

$$+ \frac{d(\text{O})}{dt} = -5k_1(\text{HCl})(\text{O}) \quad (25)$$

Integrating this expression yields -

$$\ln(\text{O}) = -5k_1(\text{HCl})t + \ln(\text{O})_0 \quad (26)$$

With $t = \text{time} = \frac{z}{u}$, $z = \text{reactor distance}$, and $u = \text{linear flow velocity}$,

$$\ln(\text{O}) = -5k_1(\text{HCl})\frac{z}{u} + \ln(\text{O})_0 \quad (27)$$

Therefore, a plot of $\ln(\text{O})$ vs. z should yield a straight line. Figure 2 shows the experimental data plotted in this manner. The reaction exhibits first-order behavior between 100 and 300 mm, but deviates from this behavior beyond this point. It almost appears that the reaction stops shortly beyond the 300-mm point. Our analysis will concentrate on the first 300 mm of the reactor. In this region the slope of the curve yields a rate constant of 2.65×10^{-15} cu cm/particle-sec. If this reaction has a steric factor of 0.1, the activation energy is about 5 kcal/g-mole.

This value for the rate constant is consistent with the postulated mechanism. The rate expression for O atom disappearance (Equation 25) shows that Reaction 1 is the slowest or rate-controlling step of the mechanism. Comparison of the value of $k_1(2.65 \times 10^{-15})$ with the values in Table II shows that this is indeed the case.

Equation 23 for the formation of CO can be simplified by applying the values of the rate constants and the various concentrations:

$$\frac{d(\text{CO})}{dt} = k_1(\text{O})(\text{HCl}) \quad (28)$$

Substituting the expression for the O atom concentration yields -

$$\frac{d(\text{CO})}{dt} = k_1(\text{HCl})(\text{O})_0 e^{-5k_1(\text{HCl})t} \quad (29)$$

Integrating Equation (29) yields -

$$(\text{CO}) = \frac{(\text{O})_0}{5} [1 - e^{-5k_1(\text{HCl})\frac{z}{u}}] \quad (30)$$

The rate expression for CO₂ can now also be integrated:

$$(\text{CO}_2) = \frac{0.4k_1k_6}{k_2} (\text{HCl})(\text{O})_0 \left[t + \frac{e^{-5k_1(\text{HCl})t} - 1}{5k_1(\text{HCl})} \right] \quad (31)$$

The integrated expressions show the correct qualitative details for the reaction, but the quantitative predictions are not accurate. For example, the equations

predict that CO should be present in greater concentrations than CO₂. Figure 3 shows that this effect is indeed observed. However, the quantitative predictions are not in agreement; the predicted rates of formation are too low.

Another qualitative feature of the reaction is shown in Figure 4. The amount of CO formed increases by a factor of 5 (in the early stages of the reaction) as the initial HCl concentration is increased. This is predicted by Equation (30).

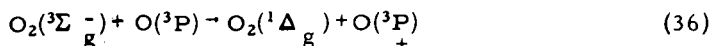
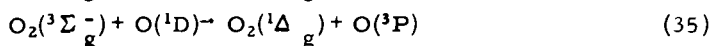
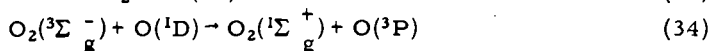
The equations predict the qualitative but not the quantitative features of the experimental data. The data quality has been determined from a mass balance on the reactants and products. About 80% of the O atoms that react are recovered as either CO or CO₂. The reaction also forms water and molecular oxygen. The amount of water is quite small and the amount of O₂ formed is also small and cannot be accurately determined because of the large background O₂ concentration. Within these limitations, the mass balance is good and indicates that the data are internally consistent. From this, it appears that the reaction scheme is incomplete.

The most probable discrepancy in the proposed scheme is the elimination of Reaction (9). This reaction can be rapid if the concentration of H atoms is sufficiently high. H atoms are formed by Reactions (2) (a very fast reaction), (5), and (6). Therefore, they may be present in a sufficiently high concentration to make Reaction (9) significant. Reaction (9) produces both CH₃ and OH radicals. CH₃ reacts, via CH₂, to form CO, and the CO is oxidized to CO₂ by OH. Hence, inclusion of Reaction (9) should provide for faster rates of CO and CO₂ formation.

B. Possible Influence of Excited O₂

The above data shows that about 25% of the original methane will be converted to products (CO + CO₂) over a reaction zone length of 350 mm. Figure 5 presents some data for this system, comparing the reaction of discharged O₂ with CH₄ to that of O atoms generated in the titration of NO with N atoms. Curve A indicates the formation of CO₂ from a CH₄/HCl mixture using O atoms generated in the gas-phase titration: N + NO → N₂ + O. Curve B gives the data for the same system after adding about 15 X 10⁻³ mm Hg of ground-state O₂ to the atom stream, which also contains about 15 X 10⁻³ mm Hg of O atoms as determined by the gas-phase titration. Discharged O₂ (with about 15 X 10⁻³ mm Hg of O atoms and 15 X 10⁻³ mm of Hg of O₂) used in place of the O atom stream obtained by titration yields Curve C, which shows considerable enhancement of the combustion process over Curves A and B. The data of Curves A and B lend support to the possibility of a specific effect of molecular oxygen on O atom reactions; excited-state molecular O₂ may be the chemically perturbing agent for these systems.

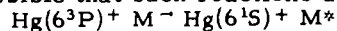
The only difference between Curves C and B is that the former presents data for the CH₄/HCl/O system in the presence of excited molecular O₂, while the latter involves only added ground-state O₂. In an electrical discharge, the following processes can take place:



The radiative loss rate constant for O₂(¹Σ⁺) may be as large as 10⁻¹³cc/particle-sec. and 10⁻²²cc/particle-sec. for O₂(¹Δ_g),⁸ thus allowing O₂(¹Δ_g) to interfere in chemical reaction systems at moderate ⁸ to rapid flow rates.⁷ ⁸ (Although quite

7. A. M. Falick and B. H. Mahan, *J. Chem. Phys.* 47, 4778 (1967).
inert toward saturated hydrocarbons, O₂(¹Δ_g) is known to react readily with atoms, free-radicals, and unsaturated compounds.)⁸

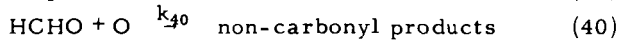
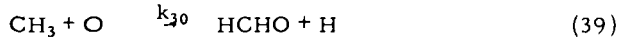
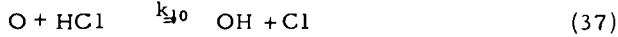
It is also possible that such reactions as



may occur in systems manometered with mercury, this effect should be observable regardless of the type of discharge used. Preliminary indications show that (37) is not significant in our system.

C. Detection of Carbonyls in CH₄-O atom Reactions

Our flow system provides for a "residence time-to-reaction length" ratio of $t/z = u^{-1} \approx 1$ msec/cm. (The linear flow rate is about 10 meters/sec.) The kinetic data points are usually spaced 10 cm apart. Therefore, any formaldehyde originally formed in the reaction of methyl radicals with O atoms must be reduced to a concentration lower than the detectable limit (about 1.60×10^{13} molecules/cu cm in this case) within 0.01 sec. The problem of HCHO formation can then be demonstrated by a crude estimate employing the following simplified steady-state scheme:



$$\frac{d[\text{Cl}]}{dt} = \frac{d[\text{CH}_3]}{dt} = \frac{d[\text{HCHO}]}{dt} = 0 \quad (41)$$

Then,

$$[\text{Cl}] = \frac{k'_{10}[\text{O}][\text{HCl}]}{k_{20}[\text{CH}_4]} \quad (42)$$

$$[\text{CH}_3] = \frac{k_{20}[\text{CH}_4][\text{Cl}]}{k_{30}[\text{O}]} \quad (43)$$

$$[\text{HCHO}] = \frac{k_{30}[\text{O}][\text{CH}_3]}{k_{40}[\text{O}]} = \frac{k_{30}}{k_{40}}[\text{CH}_3] \quad (44)$$

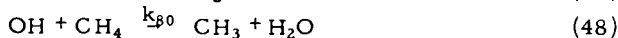
Thus,

$$[\text{HCHO}] = \frac{k'_{10}}{k_{40}}[\text{HCl}] \quad (45)$$

With $[\text{HCHO}] = 0.5$ millitorr and $[\text{HCl}] = 20$ millitorr, and with an estimated $k'_{10} \approx 10^{-12}$ cu cm/mole-sec, the most reliable data for Reaction 40 yields a value $k_{40} \approx 8 \times 10^{-13}$ cu cm/mole-sec, which would make the steady-state value of $[\text{HCHO}] \approx 25$ millitorr, an amount readily detectable by the 3015 TOF. In short, if carbonyls are intermediates in the reaction of CH₄ with O atoms at room temperature, our results demand that they be present as reactive species (such as formyl radicals, HCO) rather than stable molecules.

D. Reaction of OH with CH₄

The primary scheme associated of OH radicals in the flow reactor is as follows:



(The initial reaction to produce OH has $k_5 \gg k_6, k_7,$ and $k_8,$ and hence the conversion of H into OH is considered to be instantaneous.) In the absence of methane, the k_8 step is noncontributing and -

$$\text{Rate}(\text{OH}) = + \frac{d[\text{OH}]}{dt} = -k_{60}[\text{OH}]^2 - k_{70}[\text{O}][\text{OH}] - \gamma_{\text{OH}}[\text{OH}] \quad (50)$$

Since k_{60} and k_{70} are comparable at room temperature, we may assume a steady-state condition for O atoms such that $d[\text{O}]/dt = 0$. This yields $k_{70}[\text{O}] = k_{60}[\text{OH}]$ and hence,

$$\text{Rate}(\text{OH}) = \frac{d[\text{OH}]}{dt} = -2k_{60}[\text{OH}]^2 - \gamma_{\text{OH}}[\text{OH}] \quad (51)$$

In the presence of CH_4 , k_{80} contributes and, assuming that CH_4 does not alter the kinetic wall behavior of OH ,

$$\text{Rate}_{(\text{CH}_4, \text{OH})} = \frac{d[\text{OH}]}{dt(\text{with CH}_4)} = -2k_{60}[\text{OH}]^2 - (k_{80}[\text{CH}_4] + \gamma_{\text{OH}})[\text{OH}] \quad (52)$$

Both Equations 17 and 18 are of the form -

$$\frac{dy}{dt} = -y(ay + b) \quad (53)$$

(with $y = [\text{OH}]$) which may be solved by the substitution -

$$\mu = \frac{y}{ay + b} \quad (54)$$

which yields

$$\frac{\mu}{\mu_0} = e^{-bt} \quad (55)$$

$[\text{CH}_4]$ is assumed essentially constant since its concentration is 59 times greater than $[\text{OH}]$ in this system.

Figure 6 presents some recent data on the fast-flow reaction between CH_4 and OH . (\square indicates the reaction without CH_4 ; \circ indicates the reaction in the presence of CH_4 .)

In this system, $k_{80} \ll 2k_{60}$ and $(k_{80}[\text{CH}_4] + \gamma) \ll 2k_{60}[\text{OH}]$. These numerical values make it difficult to use the method of initial rates to analyze the data. However, it is possible to use the integrated rate equation (55). This equation can be simplified by expanding the exponential term, e^{-bt} , as a power series, neglecting the higher powers of bt since they are much less than unity:

$$\frac{y_0/(y_0 + b)}{y/(ay + b)} \approx 1 + \left(\frac{b}{vz}\right) z = 1 + bt \quad (56)$$

or rearranging Equation (56) yields -

$$y^{-1} \approx \left[\frac{1}{v} (a + by_0^{-1})\right] z + y_0^{-1} \quad (57)$$

Thus, a plot of y^{-1} against z (reciprocal of $[\text{OH}]$ versus distance, z , from inlet) should be linear. From the difference in slopes of two such straight lines (one for a run with CH_4 , one for a run without it) one can obtain k_4 , the rate constant in question. The data plotted in Figure 7 show the predicted linear relation.

From Equation 57, the definitions of a , b , and y , and setting $\text{SLOPE}_{\text{CH}_4}$ and SLOPE_0 equal to the slopes of the y^{-1} versus z curves for the run with CH_4 and the run without, respectively, yields -

$$k_{80}[\text{CH}_4] = [\text{OH}]_0(\text{CH}_4) [v_{\text{CH}_4} (\text{SLOPE}_{\text{CH}_4}) - 2k_{60}] - [\text{OH}]_0(\text{O}) [v_0(\text{SLOPE}_0) - 2k_{60}] \quad (58)$$

From Figure 10 and the 3015 sensitivity value for OH (1.60×10^{13} particles/cu cm = 10 units), and using the reported value⁶ for k_{60} (2.5×10^{-12} cu cm/part-sec) we have -

$$2k_{60} = 80 \text{ unit}^{-1} \text{ sec}^{-1}$$

$$[\text{OH}]_b(\text{CH}_4) = 10 \text{ units}$$

$$[\text{OH}]_b(\text{O}) = 7.0 \text{ units}$$

$$\text{SLOPE}_{\text{CH}_4} = 0.0326 \text{ unit}^{-1} \text{ cm}^{-1}$$

$$\text{SLOPE}_0 = 0.0474 \text{ unit}^{-1} \text{ cm}^{-1}$$

In the run with CH_4 , the flow rate $v_{\text{CH}_4} = 2.635 \times 10^3$ cm-sec⁻¹. Thus, $k_{80}[\text{CH}_4] = 58.94 \text{ sec}^{-1}$. Since $[\text{CH}_4] = 2.43 \times 10^{16}$ molecules/cu cm, we have $k_{80} = 2.42 \times 10^{-15}$ cu cm/particle-sec. This is roughly an order of magnitude lower than that recently reported by Greiner,⁸ and about 3 times lower than that reported by Wilson

8. N. R. Greiner, J. Chem. Phys. 46, 490 (1967).

and Westenberg.⁹ In the absence of data at other temperatures we may use the
 9. W. E. Wilson and A. A. Westenberg, "11th Symposium (International) on Com-
 bustion," Combustion Institute (1967).

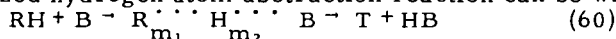
approximate collision theory argument² that the rate constant is given by -

$$k_{30} = 10^{-10} \cdot 5 e^{-E_a/RT} \quad (59)$$

which gives an activation energy of 5.65 kcal/mole for the $\text{CH}_4 + \text{OH}$ reaction.

Whether at high or low temperatures, a chain propagation step in the combustion process for a hydrocarbon is the abstraction of a hydrogen atom from the hydrocarbon by atomic oxygen or hydroxyl.

The generalized hydrogen atom abstraction reaction can be written¹⁰



10. H. S. Johnston, "Gas Phase Reaction Rate Theory," Ronald Press, New York (1966).

where m_1 and m_2 are the bond orders, in the transition state, of the "breaking bond" $\text{R} \cdot \cdot \cdot \text{H}$ and the "forming bond" $\text{H} \cdot \cdot \cdot \text{B}$. This bond-order concept has its intuitive appeal to the chemist and structural chemist on the bases of bond length, bond strength, and coordinating valence. Thus, in a single covalent bond involving one pair of shared electrons as in H_2 or HCl , the bond order is 1. In nitrogen, however, since one may see that there are three pairs contributing to bonding (a so-called " $\sigma_{2p} \pi_{4p}$ " configuration) the bond order there is 3. The important result here is to remember that, in the bimolecular reaction above, the underlying assumption is that the sum of bond orders remains constant throughout such abstraction reactions. That is, $m_1 + m_2 = 2$.

One may then treat such reactions by assuming a valence bond potential for the transition state given by

$$V = D_{\text{RH}} - C_{\text{RH}}(m_1^p) - D_{\text{HB}}(m_2^q) + V_r \quad (61)$$

where the D 's are the bond dissociation energies, V_r is the energy of repulsion arising from the parallel electron spins on R and B , and q are empirical parameters indicating the strength of the intermolecular valence forces. For oxygen species where triplet states are involved (two parallel electron spins on the same species), twice the repulsion energy has to be included for a more reasonable estimate.

Recently, our results indicated a room temperature rate constant of about 10^9 cu cm-mole⁻¹-s⁻¹ for the $\text{OH} + \text{CH}_4 \rightarrow \text{CH}_3 + \text{H}_2\text{O}$ reaction. This implies that the activation energy for such a reaction is about 5 to 6 kcal-mole⁻¹. The bond energy-bond order method yields about 5 kcal-mole⁻¹ as an activation energy.

We have also indicated that the combustion of methane is significantly enhanced in the presence of discharged rather than titrated oxygen. Our first interpretations associated this extra activity with excited O_2 , namely (Δ g) O_2 . Table III is a brief compendium of rate constants and activation energies as calculated by the bond energy-bond order method.

From the above table, it is obvious that the $\text{CH}_4 + \text{O}_2(\Delta$ g) reaction should be about 10,000 times more rapid than the ground-state O_2 reaction at flame temperatures. Although the Σ g⁺ state of O_2 indicates an even greater reaction, the lifetimes (collisional and radiative) for this species are much too short to compete with that for the Δ g state (46 minutes). Thus, no significant concentration of this Σ g⁺ species is expected. Each of the rate constants¹¹ in Table III is computed by the prescription

11. S. W. Mayer and L. Schieler, *J. Phys. Chem.* **72**, 2628 (1968).
 of activated complex theory. Successive variation of the parameters of Equation 8 leads to a "saddle point curve," or curve of steepest ascent. The maximum of this path may be taken as the activation energy, E_a . Assuming a linear complex, one can readily calculate the rate constant from

$$k_{\text{rate}} = K \frac{kT}{h} \cdot \frac{Q^\ddagger}{Q_A Q_B} e^{-E_a/RT} \quad (62)$$

where the Q_A and Q_B are reactant partition functions, Q^\ddagger is the partition function of the complex, R is the gas constant (in cal-mole⁻¹-deg⁻¹ if E_a is in cal-mole⁻¹), k is Boltzmann's constant, h is Planck's constant, and K is the transmission coefficient

for the potential barrier. Quantum mechanically, even though the energy of a system is less than the potential at that point, there is a finite probability of finding the system in the configuration beyond that point. This probability is the transmission coefficient, and the "process" is referred to as quantum-mechanical "tunnelling." In any event, Equation 62 can be readily calculated for most simple reactions and has been shown to give very reliable estimates of the rate constants for a great number of elementary reactions.

It should be observed that the reactions in Table III for $\text{CH}_4 + \text{O}_2$ are not as fast as the corresponding reactions with O atoms. However, one would expect that the reactions of $\text{O}_2(^1\Delta_g)$ with $\text{CH}_3\cdot$ radicals or with unsaturated hydrocarbon intermediates might be quite competitive with attack by oxygen atoms. For example, the best values for O atom attack on CH_4 give an activation energy of $10.5 \text{ kcal-mole}^{-1}$. However, the rate constants for reaction of O atoms with $\text{CH}_3\cdot$ may be comparable to $\text{CH}_3\cdot$ reaction with excited O_2 , since each reaction involves encounter between species having free valences. The actual concentration of excited O_2 made by an electrical discharge (concentration in the downstream effluent) may be as high as 10% of the total pressure.⁷ This would mean that in the experiments with CH_4 and HCl it would be reasonable to expect that concentrations of the order of 20 microns Hg (about 6×10^{14} molecules/cu cm) of $^1\Delta_g \text{O}_2$ were available in the reaction zone. Assuming that the reaction rates of $\text{O}_2(^1\Delta_g)$ and $\text{O}(^3P)$ atoms with CH_3 are similar, one would expect about a three-fold increase in oxidation rate in the electrical discharge experiment.

IV. Conclusions

Although both HCl (and Cl_2) catalyze the reaction of CH_4 with O and O_2 , the extent of the reaction at room temperature is small. We could detect no quantitative evidence for the formation of any carbonyls or carbonyl fragments during the course of the oxidations (this, however, does not preclude their presence as very short-lived intermediates in such systems). The presence or absence of ground-state O_2 produced no effect on the reaction of O atoms with CH_4 . Addition of O_2 to the N + NO stream gave no evidence of any rate changes. Discharged O_2 , however, significantly enhances the formation of combustion products. This result has been tentatively attributed to the presence of excited ($^1\Delta_g$) O_2 in the system. The reaction of CH_4 with OH radicals has been studied at room temperature, yielding a rate constant of $2.42 \times 10^{-15} \text{ cc/particle-sec}$.

V. Acknowledgements

The authors of this paper are deeply indebted to the American Gas Association for their support in this work.

Table I. ACTIVATION ENERGIES

<u>Reaction Number</u>	<u>Heat of Activation, kcal/g-mole</u>
(2)	4
(7)	11
(8)	8-9
(9)	8
(10)	≈ 53
(11)	≈ 58
(12)	≈ 60

Table II. RATE CONSTANTS FOR REACTIONS AT 300° K,
cu cm/particle-sec

$k_1 = \text{Unknown}$

$k_2 = 2.06 \times 10^{-11}$

$k_3 = 1.53 \times 10^{-14}$

k_4 , assumed to be between 10^{-10} - 10^{-11}

k_5 , assumed to be between 10^{-10} - 10^{-11}

$k_6 \sim 2 \times 10^{-13}$

Table III. ACTIVATION ENERGIES AND RATE CONSTANTS FOR HYDROCARBON-OXYGEN AND METHANE-OXYGEN REACTIONS (cc-mole⁻¹-sec⁻¹)

Species	$O_2(^3\Sigma_g^-)$	$O_2(^1\Delta_g)$	$O_2(^1\Sigma_g^+)$
	(Ground State)	(Excited State)	(Excited State)
	<u>With H₂</u>		
E _a	58 kcal-mole ⁻¹	35 kcal-mole ⁻¹	20 kcal-mole ⁻¹
k (300°K)	4 X 10 ⁻³⁰	1 X 10 ⁻¹⁴	1 X 10 ⁻⁶
k (1000°K)	3	3 X 10 ⁴	1 X 10 ⁵
	<u>With CH₄</u>		
E _a	57	34	19
k (300°K)	6 X 10 ⁻³⁰	4 X 10 ⁻¹⁴	2 X 10 ⁻⁶
k (1000°K)	6	6 X 10 ⁴	5 X 10 ⁶

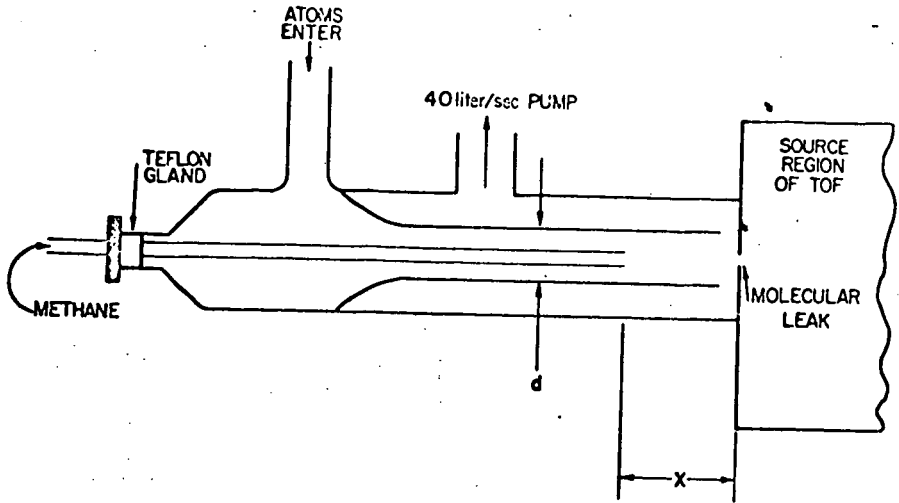


Figure 1 . FLOW REACTOR

A-1071396

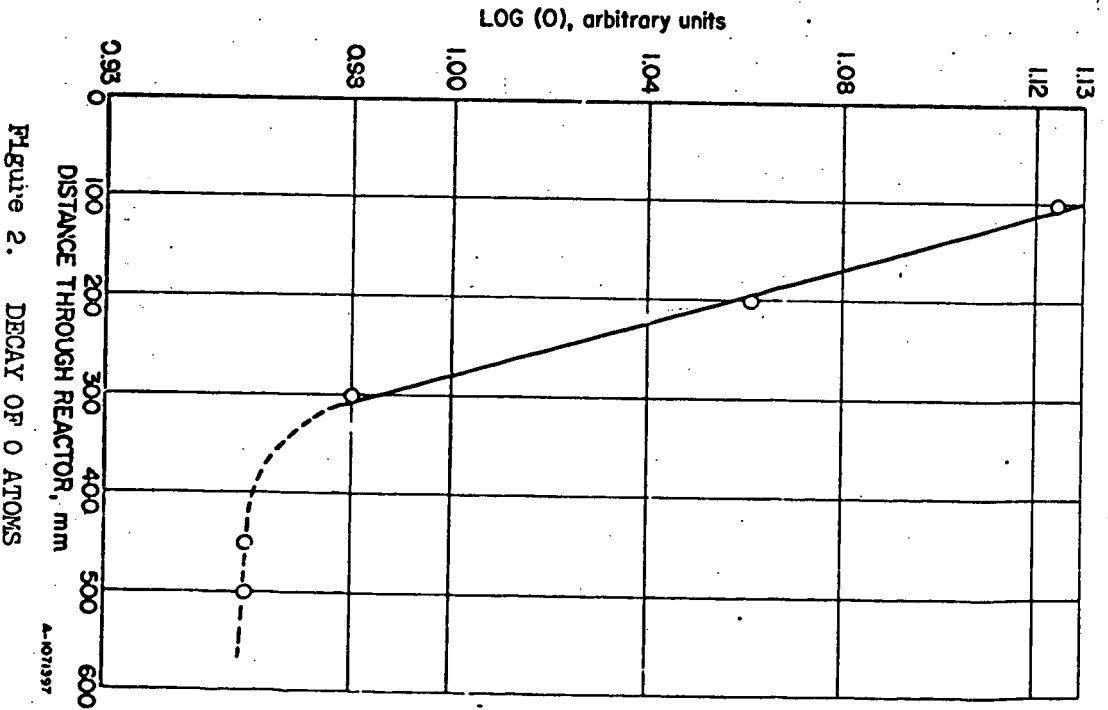
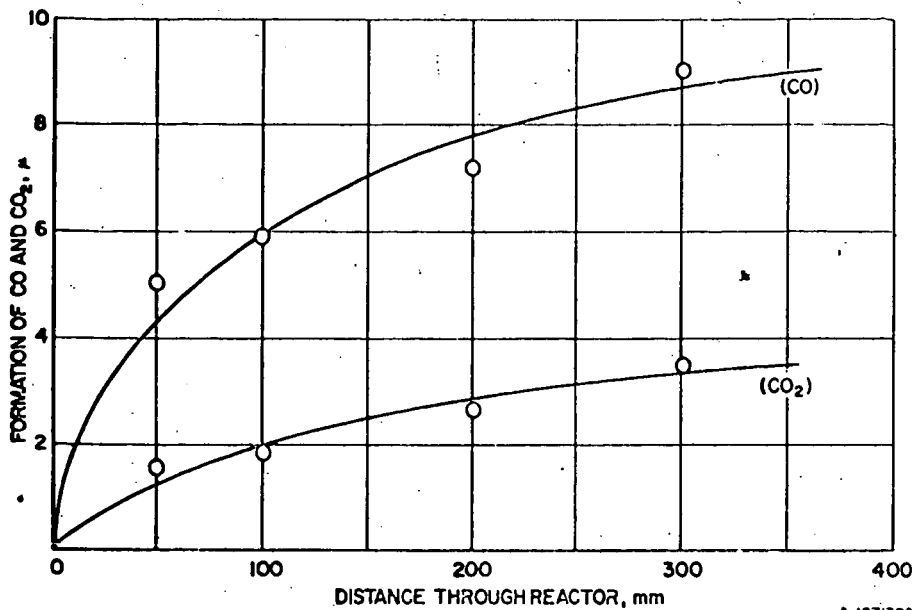


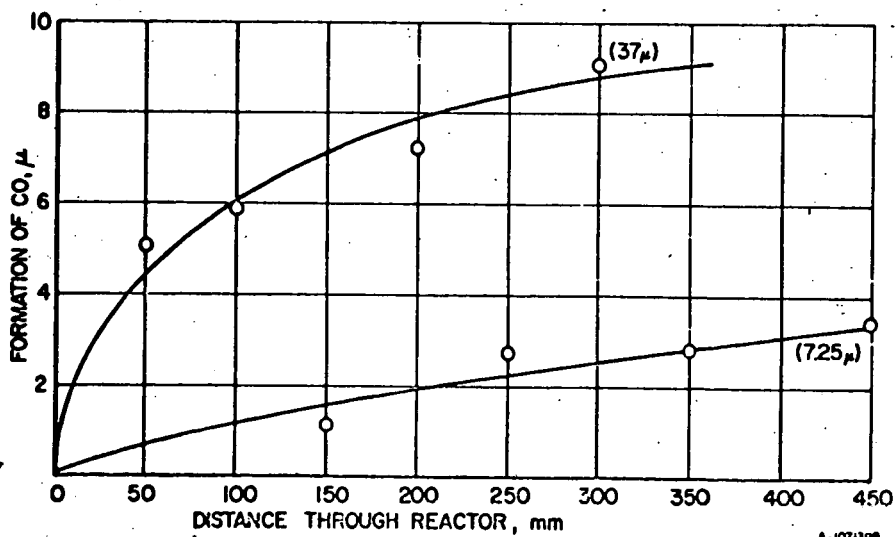
Figure 2. DECAY OF O ATOMS

A-1071397



A-1071398

Figure 3. RELATIVE FORMATION OF CO AND CO₂
WHEN 37 μ OF HCl IS ADDED



A-1071399

Figure 4. RELATIVE FORMATION OF CO FOR
DIFFERENT ADDITIONS OF HCl

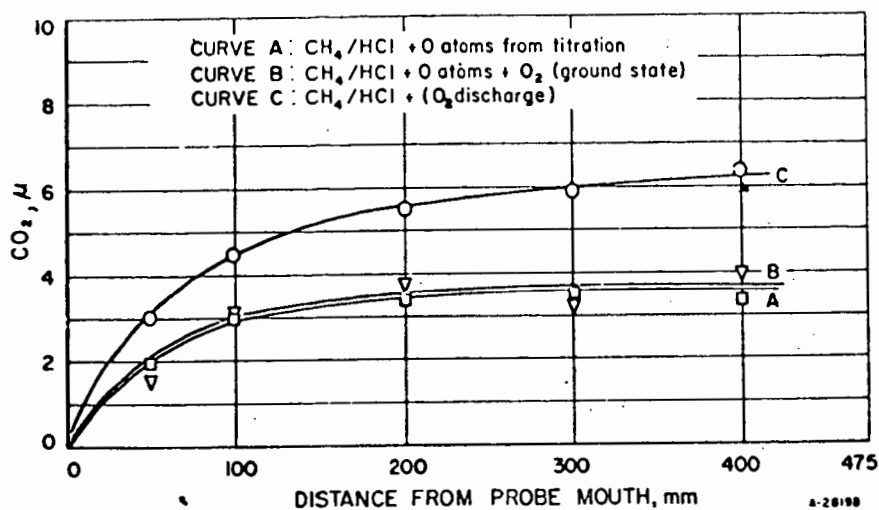


Figure 5. FORMATION OF CO_2 FOR VARIOUS $\text{CH}_4/\text{HCl}/\text{O}$ SYSTEMS

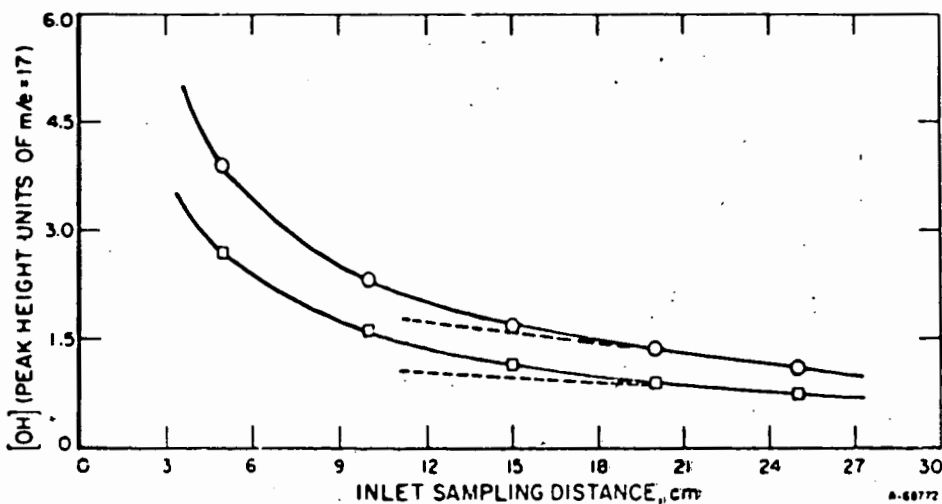


Figure 5. REACTION OF CH_4 WITH OH (at Different Initial Concentrations of OH)

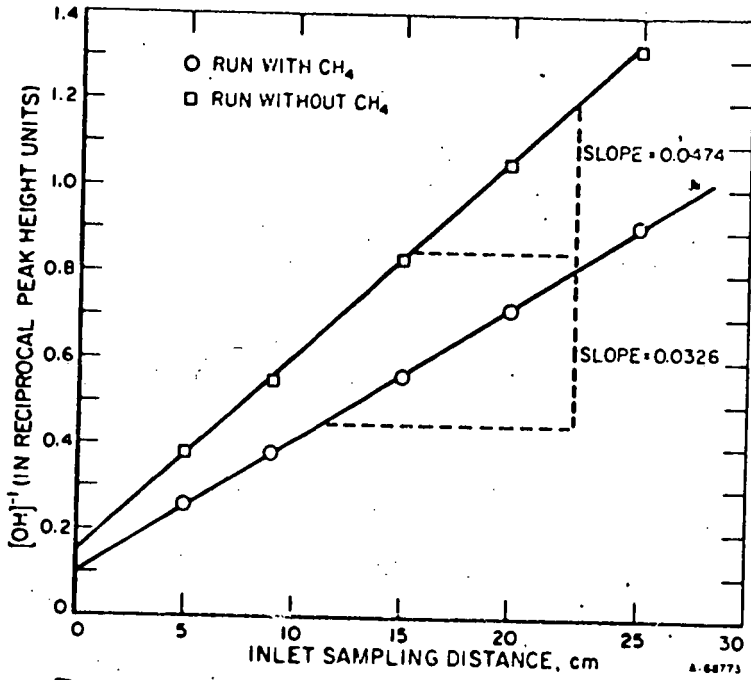


Figure 7. RECIPROCAL CONCENTRATION OF OH AS A FUNCTION OF DISTANCE FROM THE INLET DURING CH_4 -OH REACTION